

# MODELS FOR BIOMEDICAL IMAGE RECONSTRUCTION BASED ON INTEGRAL APPROXIMATION METHODS

Charles Byrne<sup>†</sup>     Dan Gordon<sup>\*</sup>     Daniel Heilper<sup>\*</sup>

<sup>†</sup>Dept. of Math. Sci., Univ. of Mass., Lowell, MA, USA. Charles\_Byrne@uml.edu

<sup>\*</sup>Dept. of Comp. Sci., Univ. of Haifa, Haifa, Israel. {gordon,dheilper}@cs.haifa.ac.il

## ABSTRACT

The most common image representation method for biomedical image reconstruction uses pixels, and the image is assumed to be constant throughout the pixel. Other methods have also been used. In many reconstruction problems, the measured data is approximated by line integrals through the object. This fact suggests a new class of model representation methods based on classical Newton-Cotes methods of integral approximations. These methods use Lagrange polynomials of one variable, and they can be extended to higher dimensions by blending. In 2D, these methods lead to the pixel model, bilinear interpolation, and higher order models. The bilinear interpolation model has been implemented and shown to be superior to the pixel model.

**Index Terms**— Basis functions, biomedical image reconstruction, integral approximation

## 1. INTRODUCTION

Biomedical image reconstruction techniques acquire physical measurements from some data acquisition process, such as CT, PET, and so on. In order to reconstruct the underlying image, the reconstruction techniques require some assumed representation for the underlying image. In two dimensions, the most prevalent method is the use of pixels, with the assumption that the value of the image is constant throughout the pixel [10].

Alternative basis functions have been proposed and implemented: splines [17], cubic B-splines [9], the sinc function [14], and modifications of the Kaiser-Bessel window functions (blobs) [12]. The latter method requires the tuning of several parameters [7]. Blobs have also been used successfully in electron tomography [6].

In two-dimensional transmission computerized tomography (CT), the measurements are approximated by line or strip integrals through the medium, and the problem is to reconstruct the value of the (unknown) density function  $f(x, y)$  from the measurements. The general framework of the reconstruction problem is to find some approximating function  $g(x, y)$  such that:

- $g(x, y)$  is represented in some simple form as a linear combination of certain basis functions;
- the line integrals through the domain are good approximations to the measurements.

In positron-emission tomography (PET), line integrals also need to be approximated. Here, the line integrals are evaluated on the line-of-response (LOR), which is the line along which two opposing photons move when a positron collides with an electron [4].

There are many different types of algorithms for image reconstruction [2, 10, 13]. Some are based on the fast Fourier transform (FFT), while others, such as ART [11, 8], are iterative. Several methods strive to satisfy some optimization criterion, such as least squares minimization [1], or expectation maximization (EM) [5]. However, even the “best” algorithms cannot derive more information from the measurements if the underlying model of data representation is lacking.

This paper contributes to the field of data representation by exploring new models. Since the approximation of line integrals is fundamental to many image reconstruction problems, it is proposed to use basis functions that are derived from standard integral approximations. Three well known rules for integral approximation are the rectangle rule, the trapezoidal rule, and Simpson’s rule. When the integral is evaluated over a finite interval  $[a, b]$ , the interval is subdivided into subintervals of uniform length  $h$ . The error of the above-mentioned approximation methods are, respectively,  $O(h)$ ,  $O(h^2)$ , and  $O(h^4)$ . These three basic rules are examples of the Newton-Cotes formulae for numerical integration [16, §3.1], which are based on Lagrange basis polynomials.

Our approach consists of using the Lagrange polynomials of one variable as *blending functions* in order to produce basis functions of higher dimension; this is a well-known technique from the field of spline approximations. Blending functions for higher dimensions are obtained by taking all possible products of the one-dimensional functions. For example, if  $f(x)$  and  $g(x)$  are the two basis functions in one dimension, then the 2D functions obtained by blending will be  $f(x)f(y)$ ,  $f(x)g(y)$ ,  $g(x)f(y)$  and  $g(x)g(y)$ . This approach can be extended to higher dimensions. For biomedical image reconstruction, the main interest will be two and three dimensions, and also four dimensions for temporal image reconstruction.

## 2. THE THREE INTEGRAL APPROXIMATION METHODS AND THE DERIVED 2D MODELS

### 2.1. The step function approximation and the pixel model

In the pixel model, assume that  $b_i$ ,  $1 \leq i \leq m$ , are the ray readings, and  $x_j$ ,  $1 \leq j \leq n$ , are the (unknown) pixel values. This gives us a system of equations  $Ax = b$ , where each coefficient  $a_{ij}$  is simply the length of the intersection of the  $i$ th ray with the  $j$ th pixel.

The pixel model is based on the step function  $s(x) = 1$ , defined over  $[0, 1]$ . By blending  $s(x)$  in 2D, we get  $s(x)s(y)$ , and it is quite easy to see that this leads to the pixel model; we omit the details.

### 2.2. The trapezoidal rule and the linear model

In this model, we will assume that the unknown values are assigned to the grid points. The model is based on the trapezoidal rule for integral approximation, as follows. Suppose  $f(x)$  is defined on an interval  $[a, b]$ . We divide  $[a, b]$  into  $n$  subintervals of equal length:

$$a = a_0 < a_1 < \dots < a_n = b,$$

and denote  $h = (b - a)/n$ . For  $0 \leq i \leq n - 1$ , let  $g_i = f(a_i)$ .

In the trapezoidal rule, the approximating function over the subinterval  $[a_i, a_{i+1}]$  is the line connecting the points  $(a_i, g_i)$  and  $(a_{i+1}, g_{i+1})$ . Linear interpolation can be represented by the use of two linear functions,  $\ell_0(x)$  and  $\ell_1(x)$  defined over  $[0, 1]$  by specifying their values at the end points:

$$\ell_0(0) = 1, \ell_0(1) = 0, \ell_1(0) = 0, \ell_1(1) = 1.$$

This yields

$$\ell_0(x) = 1 - x, \quad \ell_1(x) = x.$$

$g(x)$ , the linear interpolation approximation to  $f(x)$ , is defined (for  $a_i \leq x < a_{i+1}$ ) as

$$\begin{aligned} g(x) &= g_i \left(1 - \frac{x - a_i}{h}\right) + g_{i+1} \left(\frac{x - a_i}{h}\right) \\ &= g_i \ell_0 \left(\frac{x - a_i}{h}\right) + g_{i+1} \ell_1 \left(\frac{x - a_i}{h}\right) \end{aligned}$$

Therefore, over  $[a, b]$ ,  $g(x)$  is given by

$$g(x) = \sum_{i=0}^{n-1} \left[ g_i \ell_0 \left(\frac{x - a_i}{h}\right) + g_{i+1} \ell_1 \left(\frac{x - a_i}{h}\right) \right].$$

By blending  $\ell_0$  and  $\ell_1$  in 2D, we get four basis functions

$$\begin{aligned} \ell_{0,0}(x, y) &= \ell_0(x)\ell_0(y), \quad \ell_{0,1}(x, y) = \ell_0(x)\ell_1(y), \\ \ell_{1,0}(x, y) &= \ell_1(x)\ell_0(y), \quad \ell_{1,1}(x, y) = \ell_1(x)\ell_1(y). \end{aligned}$$

For simplicity, the 2D exposition will deal with the unit square  $0 \leq x, y \leq 1$ . Suppose  $f(x, y)$  has values  $v_i$ ,  $1 \leq i \leq$

4, on the four corners of the unit square, taken in the order  $(0, 0)$ ,  $(1, 0)$ ,  $(0, 1)$ ,  $(1, 1)$ ; see Fig. 1. The bilinear interpolation approximation of  $f$  in the unit square is

$$\begin{aligned} g(x, y) &= v_1 \ell_{0,0}(x, y) + v_2 \ell_{1,0}(x, y) + \\ &\quad v_3 \ell_{0,1}(x, y) + v_4 \ell_{1,1}(x, y). \end{aligned}$$

We shall now show how a line integral of  $g$  provides us with the coefficients of  $v_i$ . There are two types of such lines: one type intersects the square at two adjacent edges, and the other intersects it at two opposite edges. Assume that the line is of the first type, as shown in Fig. 1.

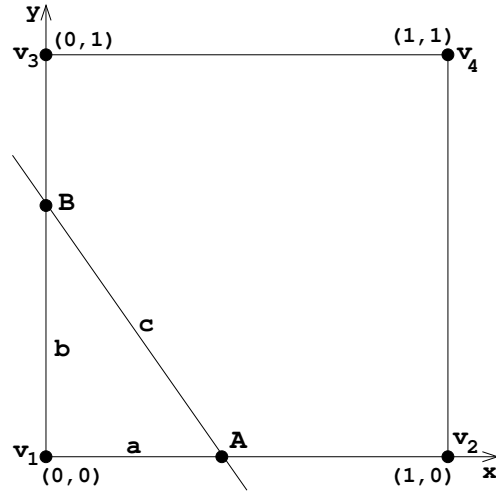


Fig. 1. Computing the line integral in the linear model.

Let  $a, b, c$  be the distances as shown in Fig. 1, and let  $s$  be a variable measuring the distance along the line from point  $A$  to point  $B$ . To get the required coefficients, we need to evaluate the line integral  $\int_0^c g(x(s), y(s)) ds$ , where  $x(s)$  and  $y(s)$  are the  $x$  and  $y$  coordinates of a point on the line  $AB$  whose distance from  $A$  is  $s$ . We now have

$$\begin{aligned} \int_0^c g(x(s), y(s)) ds &= \int_0^c \left[ v_1 \ell_{0,0}(x, y) + \right. \\ &\quad \left. v_2 \ell_{1,0}(x, y) + v_3 \ell_{0,1}(x, y) + v_4 \ell_{1,1}(x, y) \right] ds. \end{aligned}$$

For exposition, we will just evaluate the coefficient of  $v_3$ , which we denote by  $I_3$ :

$$\begin{aligned} I_3 &= \int_0^c \ell_{0,1}(x(s), y(s)) ds \\ &= \int_0^c \ell_0(x(s)) \ell_1(y(s)) ds \\ &= \int_0^c (1 - x(s)) y(s) ds. \end{aligned}$$

Referring to Fig. 1, it is easy to see that  $x(s) = a(1 - s/c)$

and  $y(s) = bs/c$ , from which we get

$$\begin{aligned} I_3 &= \int_0^c \left(1 - a \left(1 - \frac{s}{c}\right)\right) \times \frac{bs}{c} ds \\ &= \dots = \frac{bc(3-a)}{6}. \end{aligned}$$

The final coefficient of every  $v_i$ , in the equation corresponding to a given line, will be the sum of similar expressions from adjacent pixels intersected by the same line; these expressions will be added together to form the final coefficient. For example, the final coefficient of  $v_3$  in the equation corresponding to the line in Fig. 1 will be the sum of two or three expressions from adjacent pixels:  $I_3$  (evaluated above), plus the expression for  $v_3$  evaluated from the pixel to the left, plus possibly a similar expression from a third pixel (depending on how the line intersects the pixel above and to the left).

### 2.3. Simpson's rule and the quadratic model

Simpson's rule for integral approximation is based on the following three quadratic basis functions defined over  $[0, 2]$ :

$$\begin{aligned} q_0(x) &= \frac{1}{2}x^2 - \frac{3}{2}x + 1 \\ q_1(x) &= -x^2 + 2x \\ q_2(x) &= \frac{1}{2}x^2 - \frac{1}{2}x \end{aligned}$$

In 2D, we get nine basis functions defined over  $[0, 2] \times [0, 2]$  by blending:  $q_{ij}(x, y) = q_i(x)q_j(y)$ , for  $0 \leq i, j \leq 2$ . The computation of the equation coefficients will be more complicated than in the previous case, and they will depend on the geometry of the intersection of the line with a  $2 \times 2$  square of pixels (there are five types of such intersections).

## 3. RESULTS AND DISCUSSION

The linear model was implemented in 2D within the framework of the SNARK09 image reconstruction software package [15]. A phantom image of size  $95 \times 95$  pixels was created using a total of 27 elliptic shapes of various sizes. The reconstruction geometry consisted of 95 parallel uniform lines at a spacing of one pixel apart, with 95 equally spaced angles. Reconstruction was done with ART (algebraic reconstruction technique), which is actually the Kaczmarz algorithm [11], but independently rediscovered in the context of image reconstruction from projections [8]. A relaxation parameter of 0.05 was used in all iterations. It is well known that ART with a small relaxation parameter provides good images [10], and the result is very close to the least squares solution [3].

Fig. 2 shows the relative error of the two reconstructions, as compared to the phantom. The pixel model reaches a minimum relative error of 0.0489 at 17 iterations, while the linear model reaches a minimum of 0.0398 at 12 iterations. The difference between the plots may not seem great, but the *relative* difference is significant. For example, at five iterations, the

relative error of the pixel model is larger than that of the linear model by 36%. These differences are clearly noticeable in the resulting images in Fig. 3. Note in particular the central area, and the bottom right white ellipse.

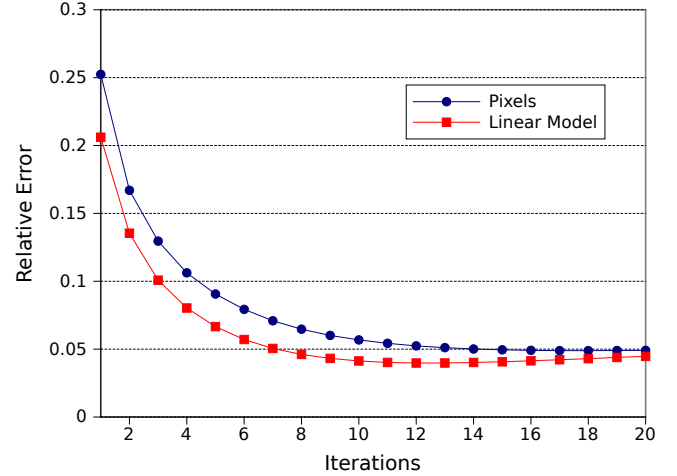


Fig. 2. Relative error plot of the pixel and linear models.

## 4. CONCLUSIONS

A new data representation model for biomedical image reconstruction was introduced. It is based on classical Newton-Cotes techniques for integral approximation, such as the rectangle rule, the trapezoidal rule, and Simpson's rule. The model based on the trapezoidal rule was implemented and shown to be superior to the standard pixel model.

Clearly, more work is required to fully evaluate the new class of data representation. The following are some additional topics for further research:

- Comparisons with other data models, such as blobs.
- Tests with various types of data, including clinical sinograms, noisy and/or low contrast data, and limited measurements (resulting in underdetermined linear systems).
- Experiments with other reconstruction algorithms.
- Examination of the quadratic model (based on Simpson's rule), which can be expected to provide even better results.
- Fully 3D reconstructions.
- Applications to PET and electron tomography.
- Experiments with other integral approximation methods, such as Gauss-Kronrod and Clenshaw-Curtis.

## 5. REFERENCES

- [1] E. Artzy, T. Elfving, and G. T. Herman. Quadratic optimization for image reconstruction, II. *Comput. Graph. & Im. Proc.*, 11:242–261, 1979.

- [2] C. L. Byrne. A unified treatment of some iterative algorithms in signal processing and image reconstruction. *Inverse Prob.*, 20:103–120, 2004.
- [3] Y. Censor, P. P. B. Eggermont, and D. Gordon. Strong underrelaxation in Kaczmarz’s method for inconsistent systems. *Numerische Mathematik*, 41:83–92, 1983.
- [4] M. Defrise and P. Kinahan. Ch. 2: Data acquisition and image reconstruction for PET. In B. Bendriem and D. W. Townsend, editors, *The Theory and Practice of 3D PET*, pages 11–54. Springer, 1998.
- [5] A. P. Dempster, N. M. Laird, and D. B. Rubin. Maximum likelihood from incomplete data via the EM algorithm. *J. Royal Stat. Soc., Ser. B*, 39(1):1–38, 1977.
- [6] J.-J. Fernández, D. Gordon, and R. Gordon. Efficient parallel implementation of iterative reconstruction algorithms for electron tomography. *J. Parallel Distrib. Comput.*, 68(5):626–640, May 2008.
- [7] E. Garduño and G. T. Herman. Optimization of basis functions for both reconstruction and visualization. *Discrete Appl. Math.*, 139:95–111, 2004.
- [8] R. Gordon, R. Bender, and G. T. Herman. Algebraic reconstruction techniques (ART) for three-dimensional electron microscopy and X-ray photography. *J. of Theor. Biol.*, 29(3):471–481, Dec. 1970.
- [9] K. M. Hanson and G. W. Wecksung. Local basis-function approach to computed tomography. *Applied Optics*, 24(23):4028–4039, 1985.
- [10] G. T. Herman. *Fundamentals of Computerized Tomography: Image Reconstruction From Projections*. Springer, 2nd edition, 2009.
- [11] S. Kaczmarz. Angenäherte Auflösung von Systemen linearer Gleichungen. *Bulletin de l’Académie Polonaise des Sciences et Lettres*, A35:355–357, 1937.
- [12] S. Matej and R. M. Lewitt. Practical considerations for 3-D image reconstruction using spherically symmetric volume elements. *IEEE Trans. Med. Imaging*, 15:68–78, 1996.
- [13] F. Natterer and F. Wübbeling. *Mathematical methods in image reconstruction*. SIAM, Philadelphia, PA, 2001.
- [14] H. M. Shieh and C. L. Byrne. Image reconstruction from limited Fourier data. *J. Opt. Soc. Am. A.*, 23:2732–2736, 2006.
- [15] SNARK09. <http://www.snark09.com>.
- [16] J. Stoer and R. Bulirsch. *Introduction to Numerical Analysis*. Springer-Verlag, New York, 1980.
- [17] M. Unser. Splines: a perfect fit for signal and image processing. *IEEE Signal Proc. Mag.*, 16(6):22–38, Nov. 1999.

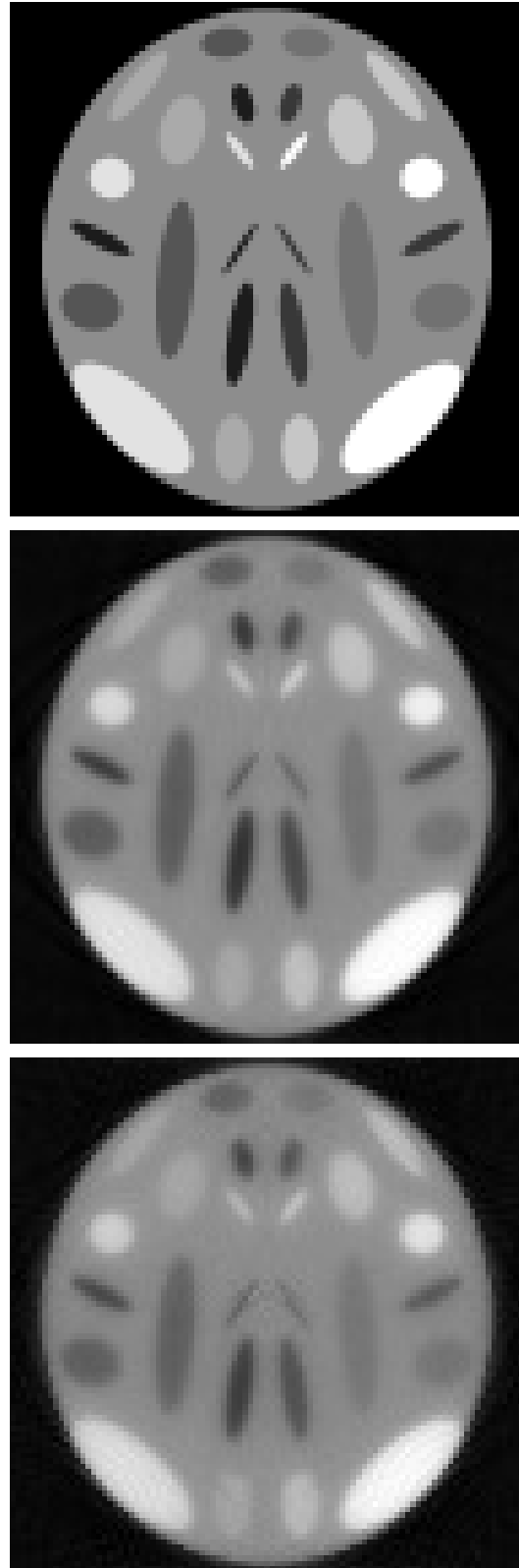


**Fig. 3.** Top to bottom: phantom, linear and pixel results after five iterations.